doi:10.3772/j.issn.1006-6748.2014.04.014

Dynamic analysis of double racks gear 3D roll forming machine①

Na Risu (那日苏)*, Li Qiang②**, Guan Yanzhi**, Yan Yu**
(*College of Mechanical Engineering, Inner Mongolia University of Technology, Hohhot 010051, P. R. China)
(**College of Mechanical and Electrical Engineering, North China University of Technology, Beijing 100144, P. R. China)
(***College of Sciences, Inner Mongolia University of Technology, Hohhot 010051, P. R. China)

Abstract

3D roll-forming for high strength steel sheets is a new technology at present. Double racks gear 3D roll forming machine developed by our research group can be used to perform variable cross section roll forming for high strength steel. In the paper, a dynamic model of 8-DOF double rack gear 3D roll-forming machine is established by the method of Lagrange equation. The expression of the angle acceleration of the system response is obtained by solving the dynamic equations. Through an actual engineering example, the dynamical characters of the 3D roll forming machine are revealed. The results can support the design of 3D roll forming machine. Meanwhile, the research will play an active role in the development of control system.

Key words: ultra high strength steel, 3D roll-forming machine, dynamic analysis, variable cross section

0 Introduction

In cold-roll forming, a metal sheet is fed through forming rolls successively until it is formed into some desired cross-sectional profile[1]. As known, a traditional roll forming machine can only produce a profile with invariable longitudinal cross-section. Besides, variable cross section roll forming, as a kind of advanced and applicable new technology of net-shape forming process, can produce variable section parts to match the loads distribution along longitudinal direction so as to keep the stress changed constantly. Variable cross section roll forming can also get the best performance of sectional mechanical properties because it can not only reduce the amount of materials, but also improves loading capability of parts, which can be realized by sequence coordinated movement of 3D roll forming machine with 3 dimensions axis linkage movement of roller groups on each stand. A new kind of double racks gear 3D roll forming machine which has been developed by our group is shown in Fig. 1, which is feasible to produce variable cross section roll forming parts for cars and constructions.

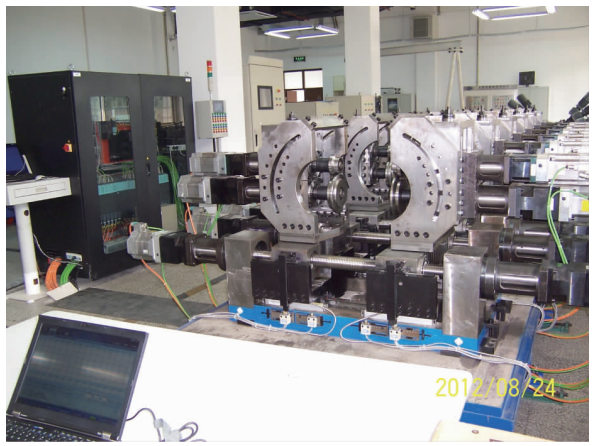

Fig. 1 Double racks gear 3D roll forming machine

In previous years some researchers investigated the roll forming process using the finite element method. In most cases, however, these studies only focused on the distribution of stress and strains in the formed profiles. For instances, Larra˜Naga1, et al.[2] developed the finite element model of three conventional stand roll forming prototype to simulate the roll forming process where friction was taken into account. 3D finite element modellings of the roll forming for a V-section profile by Paralikas, et al.[3], U-profile by Bui QV and Ponthot[4], W-bends, square pipe and multi-stands by Kim and Oh[5] were successfully established to characterize the influence of different roll-forming parameters. And other researchers[6,7] further studied on the 3D simulation to prove that the dynamic explicit FEM code in the PAM-STAMP or ANSYS/LS-DYNA environment was a more useful simulation for the roll

① Supported by the National Science and Technology Supporting Plan Projects of China (No. 2011BAG03B03).
② To whom correspondence should be addressed. E-mail: liqiang3736@qq.com
Received on Sep. 30, 2013

forming process with more complex shape. Cai, et al. [8] discussed in detail the mechanism of the three-dimensional surface formation in continuous sheet metal forming process in the longitudinal and transverse directions. Furthermore, the longitudinal strain on the edge of the strip, per roll station, along the roll forming direction and shear in the strip's plane was investigated by Paralikas, et al. [9] to optimize the roll forming process. A general method for predicting the manufacturing residual stresses and plastic strains in cold-formed steel members was developed[10], the optimization design of cold roll forming[11] based on the response surface method made the number of stands into the minimum without making any troubles such as edge wave.

A 3D roll forming machine provides multiple space motion, big forming force and multi-axis linkage in the procedure of sheet metal forming, where the dynamical analysis is necessary to develop a feasible control system. Dynamic equations are based on the dynamic model of the system, which establish the mathematic representation of the relationship between system input, system parameter and system states. They are usually differential equations based on the principle of mechanics[12,13].

However, due to the complexity of the 3D roll forming machine, little researches have investigated the dynamic model of it.

In this paper, therefore, in order to provide a dynamical design theory of a double racks gear 3D roll forming machine, dynamical Lagrange equations are deduced using the kinetic energy of one stand dynamical model. Based on the characteristics of high strength steel materials, elastic-plastic dynamical analysis of high strength steel sheet roll forming process is finished with the method of FEM, the mechanism of transformation of energy in the multi-physics field is revealed, and the dynamic loads of the rollers are obtained with the effect of constitutive relationship of high strength steel. In the dynamic equations, the inputs are the output of the servomotors and the loads of roller group in the roll forming process, and the outputs of the equation are angular accelerations of servo motors.

1 Motion analysis of variable cross section roll-forming machine

The 3D roll-forming machine is functioned by a double rack gear to get biaxial compound movement. Fig. 2 shows an example of certain stand dynamic model of a 3D roll forming machine.

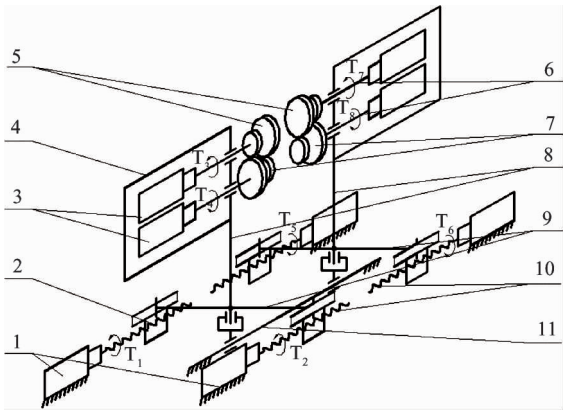

1. servo motor 2. rack 3. servo motor 4. roller frame 5. upper roller group 6. roller axis 7. down roller group 8. vertical turning axis of the frame 9. gear 10. ball screw 11. sliding guide

Fig. 2 Dynamical model of certain stand in **3**D roll forming machine

From Fig. 2, it can be seen that the lateral linear movement of roller frame 4 jointing gear 9 can be realized by synchronous motion of double rack 2, and the rotation of roller frame 4 around vertical axis can be achieved by asynchronous motion of double rack 2.

Fig. 2 also reveals that in single forming step, bilateral variable cross-section roll-forming stand includes eight degrees of freedom to meet the variable width, variable curvature cross-section roll forming, that is: the upper and lower rollers at the left and right side rotate around its self axis, the left and right side rollers move laterally and the left and right side rollers swing around the vertical axis. Ball screw 10 is driven by servo motor 1. Both sides of racks are jointed with screw seats, and mating simultaneously with gear 9. If both sides of racks move at the same speed and direction, gear 9 together with frame 4 will be driven back or forward. If both sides of racks move at the same speed and reverse direction, gear 9 and frame 4 will be driven to rotate around vertical axis of the gear. If the racks move at different speed and direction, gear 9 and frame 4 will be driven to move along transversal direction, and rotate around the axis of the gear at the same time. Meanwhile, servo motor 3 drives both the upper and lower rolls to rotate around its axis.

The rotation angle, angular velocity, and torque of left and right servo motors 3 are respectively expressed as φ_i、ω_i and $T_i(i = 1,2,3,4)$. The direction of the torque is shown in Fig. 2. The pitch of the ball screw is p, the pitch radius of gear is r, speed ratio of reducer that connects the motor shaft and the ball screw is i. As the relationship shown in Fig. 2, in the left side, straight-line velocity of the rack is $v_j = \frac{h}{2\pi}$

$\frac{\dot{\varphi}_j}{i}$ $(j = 1,2)$, the translational velocity of the gear is: $v_y = \frac{1}{2}(v_1 + v_2) = \frac{h}{4\pi i}(\dot{\varphi}_1 + \dot{\varphi}_2)$, rotation speed of gear around the axis is: $\omega_z = \frac{1}{2r}(v_1 - v_2) = \frac{h}{4\pi ri}(\dot{\varphi}_1 - \dot{\varphi}_2)$.

Because of the symmetries of structures, in the right side, the rotation angle , angular velocity and torque of four driven servo motors can be expressed as φ_i、ω_i and T_i $(i = 5,6,7,8)$. The expression of straight-line velocity and translational velocity of the rack, rotation speed of gear around the axis is obtained by replacing $j = 1,2$ with $j = 5,6$.

2 Dynamic analysis of 3D roll forming machine

The system damping forces are to be ignored because of the very large forming force. The dynamic equations are established by using energy of mechanical system in the Lagrange method, where the numbers of equations are equal to the degrees of freedom of the machine. The common expression is as follows[14]:

$$\frac{\mathrm{d}}{\mathrm{d}t}\frac{\partial L}{\partial \dot{q}_k} - \frac{\partial L}{\partial q_k} = Q_k \quad (k = 1,2,\cdots,N) \tag{1}$$

here, L is the system's kinetics, q_k is a generalized coordinate and Q_k is a generalized force.

2.1 Generalized coordinate and force

Counter-force of roller is indicated by F and torque of roller is M. The upper and lower rollers are indicated by indexes u and l, radial and axial directions are indicated by indexes r and a, horizontal axis of the roller and central axis of the gear are indicated by indexes h and v, the right and left sides of the 3D roll forming machine are indicated by indexes z and y, respectively. To set the steering angle of spindle of eight servo motors φ_i $(i = 1,2,\cdots,8)$ as generalized coordinate, based on the motion analysis of system, the expression of kinetic energy is listed as follows:

$$\begin{aligned}
2L = {} & J_{dj1}\dot{\varphi}_1^2 + J_{dj2}\dot{\varphi}_2^2 + J_{Js1}\dot{\varphi}_1^2 + J_{Js2}\dot{\varphi}_2^2 + J_{sg1}\frac{\dot{\varphi}_1^2}{i} \\
& + J_{sg2}\frac{\dot{\varphi}_2^2}{i} + J_{clz}\left(\frac{h}{4\pi ri}\right)^2(\dot{\varphi}_1 - \dot{\varphi}_2)^2 \\
& + m_{zzz}\left(\frac{h}{4\pi i}\right)^2(\dot{\varphi}_1 + \dot{\varphi}_2)^2 + J_{zzz}\left(\frac{h}{4\pi ri}\right)^2(\dot{\varphi}_1 - \dot{\varphi}_2)^2 \\
& + m_{zsz}\left(\frac{h}{2\pi i}\right)^2\dot{\varphi}_1^2 + m_{ysz}\left(\frac{h}{2\pi i}\right)^2\dot{\varphi}_2^2 \\
& + m_{xjz}\left(\frac{h}{4\pi i}\right)^2(\dot{\varphi}_1 + \dot{\varphi}_2)^2 + J_{xjz}\left(\frac{h}{4\pi ri}\right)^2(\dot{\varphi}_1 - \dot{\varphi}_2)^2 \\
& + J_{dj3}\dot{\varphi}_3^2 + J_{dj4}\dot{\varphi}_4^2 + J_{Js3}\dot{\varphi}_3^2 + J_{Js4}\dot{\varphi}_4^2 + \frac{1}{i^2}J_{uzz}\dot{\varphi}_3^2 \\
& + \frac{1}{i^2}J_{lzz}\dot{\varphi}_4^2 + \frac{1}{i^2}J_{ugz}\dot{\varphi}_3^2 + \frac{1}{i^2}J_{lgz}\dot{\varphi}_4^2 + J_{dj5}\dot{\varphi}_5^2 \\
& + J_{dj6}\dot{\varphi}_6^2 + J_{Js5}\dot{\varphi}_5^2 + J_{Js6}\dot{\varphi}_6^2 + J_{sg5}\frac{\dot{\varphi}_5^2}{i} + J_{sg6}\frac{\dot{\varphi}_6^2}{i} \\
& + J_{cly}\left(\frac{h}{4\pi ri}\right)^2(\dot{\varphi}_5 - \dot{\varphi}_6)^2 + m_{zzy}\left(\frac{h}{4\pi i}\right)^2(\dot{\varphi}_5 + \dot{\varphi}_6)^2 \\
& + J_{zzy}\left(\frac{h}{4\pi ri}\right)^2(\dot{\varphi}_5 - \dot{\varphi}_6)^2 + m_{zsy}\left(\frac{h}{2\pi i}\right)^2\dot{\varphi}_5^2 \\
& + m_{ysy}\left(\frac{h}{2\pi i}\right)^2\dot{\varphi}_6^2 + m_{xjy}\left(\frac{h}{4\pi i}\right)^2(\dot{\varphi}_5 + \dot{\varphi}_6)^2 \\
& + J_{xjy}\left(\frac{h}{4\pi ri}\right)^2(\dot{\varphi}_5 - \dot{\varphi}_6)^2 + J_{dj7}\dot{\varphi}_7^2 + J_{dj8}\dot{\varphi}_8^2 \\
& + J_{Js7}\dot{\varphi}_7^2 + J_{Js8}\dot{\varphi}_8^2 + \frac{1}{i^2}J_{uzy}\dot{\varphi}_7^2 + \frac{1}{i^2}J_{lzy}\dot{\varphi}_8^2 \\
& + \frac{1}{i^2}J_{ugy}\dot{\varphi}_7^2 + \frac{1}{i^2}J_{lgy}\dot{\varphi}_8^2
\end{aligned} \tag{2}$$

where:

- J_{dji} $(i = 1,2,\cdots,8)$ is the moment of inertia of servo-motor;
- J_{Jsi} $(i = 1,2,\cdots,8)$ is the moment of inertia of reducer connected with servo-motor;
- i is the speed ratio of servo-motor reducer;
- J_{sgi} $(i = 1,2,5,6)$ is the moment of inertia of ball screw;
- J_{clz}, J_{cly} is the moment of inertia of left and right gear;
- m_{zzz}, m_{zzy} is the mass of left and right rotating spindle;
- J_{zzz}, J_{zzy} is the moment of inertia of left and right rotating spindle;
- m_{zsz}, $m_{zsy}m_{ysz}$, m_{ysy} is the mass of left and right screw seat components;
- m_{xjz}, m_{xjy} is the mass of left and right rotating frame assembly;
- J_{xjz}, J_{xjy} is the moment of inertia of left and right rotating frame assembly;
- J_{uzz}, J_{lzz} is the moment of inertia of left upper and lower roller axle;
- J_{uzy}, J_{lzy} is the moment of inertia of right upper and lower roller axle;
- J_{ugz}, J_{lgz} is the moment of inertia of left upper and lower roller;
- J_{ugy}, J_{lgy} is the moment of inertia of right upper and lower roller;

According to the principle of virtual work, generalized force of the system can be obtained as follows:

$$Q_1 = T_1 + \frac{p}{4\pi ri}(M_{uvz} + M_{dvz}) - \frac{p}{4\pi i}(F_{uaz} + F_{daz})$$

$$Q_2 = T_2 - \frac{p}{4\pi ri}(M_{uvz} + M_{dvz}) - \frac{p}{4\pi i}(F_{uaz} + F_{daz})$$

$$
\begin{aligned}
Q_3 &= T_3 + \frac{M_{uhz}}{i}\\
Q_4 &= T_4 + \frac{M_{dhz}}{i}\\
Q_5 &= T_5 + \frac{p}{4\pi ri}(M_{uvy} + M_{dvy}) - \frac{p}{4\pi i}(F_{uvy} + F_{dvy})\\
Q_6 &= T_6 - \frac{p}{4\pi ri}(M_{uvy} + M_{dvy}) - \frac{p}{4\pi i}(F_{uvy} + F_{dvy})\\
Q_7 &= T_7 + \frac{M_{uhy}}{i}\\
Q_8 &= T_8 + \frac{M_{dhy}}{i}
\end{aligned} \tag{3}
$$

2.2 Dynamic equations and solution

If make:

$$
\begin{aligned}
J_{11} &= \frac{1}{i^2}\left[i^2J_{dj1} + i^2J_{js1} + J_{sg1} + \left(\frac{h}{4\pi r}\right)^2 J_{clz} + m_{zzz}\left(\frac{h}{4\pi}\right)^2 + J_{zzz}\left(\frac{h}{4\pi}\right)^2 + m_{zsz}\left(\frac{h}{2\pi}\right)^2 + m_{xjz}\left(\frac{h}{4\pi}\right)^2 + J_{xjz}\left(\frac{h}{4\pi r}\right)^2\right]\\
J_{22} &= \frac{1}{i^2}\left[i^2J_{dj2} + i^2J_{js2} + J_{sg2} + \left(\frac{h}{4\pi r}\right)^2 J_{clz} + m_{zzz}\left(\frac{h}{4\pi}\right)^2 + J_{zzz}\left(\frac{h}{4\pi r}\right)^2 + m_{ysz}\left(\frac{h}{2\pi}\right)^2 + m_{xjz}\left(\frac{h}{4\pi}\right)^2 + J_{xjz}\left(\frac{h}{4\pi r}\right)^2\right]\\
J_{12} &= \frac{1}{i^2}\left[J_{clz}\left(\frac{h}{4\pi r}\right)^2 + m_{zzz}\left(\frac{h}{4\pi}\right)^2 J_{zzz}\left(\frac{h}{4\pi r}\right)^2 + m_{xjz}\left(\frac{h}{4\pi}\right)^2 + J_{xjz}\left(\frac{h}{4\pi r}\right)^2\right]\\
J_{33} &= \frac{1}{i^2}[i^2J_{dj3} + i^2J_{Js3} + J_{ugz} + J_{uzz}]\\
J_{44} &= \frac{1}{i^2}[i^2J_{dj4} + i^2J_{Js4} + J_{lgz} + J_{lzz}]\\
J_{55} &= \frac{1}{i^2}\left[i^2J_{dj5} + i^2J_{js5} + J_{sg5} + \left(\frac{h}{4\pi r}\right)^2 J_{cly} + m_{zzy}\left(\frac{h}{4\pi}\right)^2 + J_{zzy}\left(\frac{h}{4\pi}\right)^2 + m_{zsy}\left(\frac{h}{2\pi}\right)^2 + m_{xjy}\left(\frac{h}{4\pi}\right)^2 + J_{xjy}\left(\frac{h}{4\pi r}\right)^2\right]\\
J_{66} &= \frac{1}{i^2}\left[i^2J_{dj6} + i^2J_{js6} + J_{sg6} + \left(\frac{h}{4\pi r}\right)^2 J_{cly} + m_{zzy}\left(\frac{h}{4\pi}\right)^2 + J_{zzy}\left(\frac{h}{4\pi r}\right)^2 + m_{ysy}\left(\frac{h}{2\pi}\right)^2 + m_{xjy}\left(\frac{h}{4\pi}\right)^2 + J_{xjy}\left(\frac{h}{4\pi r}\right)^2\right]\\
J_{56} &= \frac{1}{i^2}\left[J_{cly}\left(\frac{h}{4\pi r}\right)^2 + m_{zzy}\left(\frac{h}{4\pi}\right)^2 J_{zzy}\left(\frac{h}{4\pi r}\right)^2 + m_{xjy}\left(\frac{h}{4\pi}\right)^2 + J_{xjy}\left(\frac{h}{4\pi r}\right)^2\right]\\
J_{77} &= \frac{1}{i^2}[i^2J_{dj7} + i^2J_{Js7} + J_{ugy} + J_{dzy}]\\
J_{88} &= \frac{1}{i^2}[i^2J_{dj8} + i^2J_{Js8} + J_{ugy} + J_{dzy}]
\end{aligned} \tag{4}
$$

among which, $J_{ii}(i = 1,2,\cdots,8)$, J_{12}, J_{56} are functions of the system geometric parameters and rotational inertia of the machine components, so they are usually called equivalent moment of inertia. Bringing these parameters into Eq. (2), it's easy to get:

$$
\begin{aligned}
L = {} & \frac{1}{2}J_{11}\dot{\varphi}_1^2 + \frac{1}{2}J_{22}\dot{\varphi}_2^2 + J_{12}\dot{\varphi}_1\dot{\varphi}_2 + \frac{1}{2}J_{33}\dot{\varphi}_3^2 + \frac{1}{2}J_{44}\dot{\varphi}_4^2 + \frac{1}{2}J_{55}\dot{\varphi}_5^2 + \frac{1}{2}J_{66}\dot{\varphi}_6^2\\
& + J_{56}\dot{\varphi}_5\dot{\varphi}_6 + \frac{1}{2}J_{77}\dot{\varphi}_7^2 + \frac{1}{2}J_{88}\dot{\varphi}_8^2
\end{aligned} \tag{5}
$$

According to Eqs(1) and (2), the partial derivatives with respect to the generalized velocities are easily worked out respectively, and the dynamical differential equations can be deduced as

$$
\begin{cases}
J_{11}\ddot{\varphi}_1 + J_{12}\ddot{\varphi}_2 = T_1 + \dfrac{h}{4\pi ri}(M_{uvz} + M_{dvz}) + \dfrac{h}{4\pi i}(F_{uaz} + F_{daz})\\
J_{22}\ddot{\varphi}_2 + J_{12}\ddot{\varphi}_1 = T_2 + \dfrac{h}{4\pi ri}(M_{uvz} + M_{dvz}) + \dfrac{h}{4\pi i}(F_{uaz} + F_{daz})\\
J_{33}\ddot{\varphi}_3 = T_3 + \dfrac{M_{uhz}}{i}\\
J_{44}\ddot{\varphi}_4 = T_4 + \dfrac{M_{dhz}}{i}\\
J_{55}\ddot{\varphi}_5 + J_{56}\ddot{\varphi}_6 = T_5 + \dfrac{h}{4\pi ri}(M_{uvy} + M_{dvy}) + \dfrac{h}{4\pi i}(F_{uay} + F_{day})\\
J_{66}\ddot{\varphi}_6 + J_{56}\ddot{\varphi}_5 = T_6 + \dfrac{h}{4\pi ri}(M_{uvy} + M_{dvy}) + \dfrac{h}{4\pi i}(F_{uay} + F_{day})\\
J_{77}\ddot{\varphi}_7 = T_7 + \dfrac{M_{uhy}}{i}\\
J_{88}\ddot{\varphi}_8 = T_8 + \dfrac{M_{dhy}}{i}
\end{cases} \tag{6}
$$

In Eq. (6), with a given time dependent load of roller, expression of the angular velocity of motor can be obtained by solving the equations mentioned above.

3 Example analysis

In this study, taking the variable cross section roll forming process of 1.5mm thick TRIP600 high strength

steel sheet as an example, in the conditions of 3m/s feeding speed, dynamic finite element analysis is performed by ABAQUS, as shown in Fig. 3. For the symmetry of the 3D roll forming machine and the symmetry loads, only the left side of the 3D roll forming machine is considered.

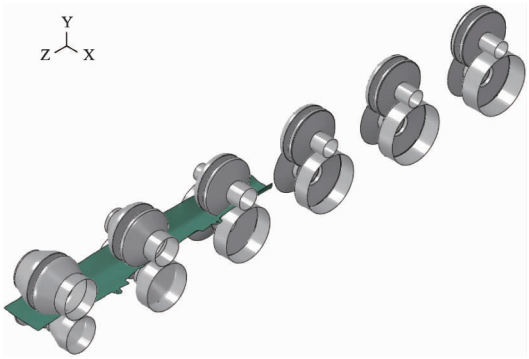

Fig. 3 Dynamic finite element analysis for the 1.5mm thick TRIP600 high strength steel sheet 3D roll forming

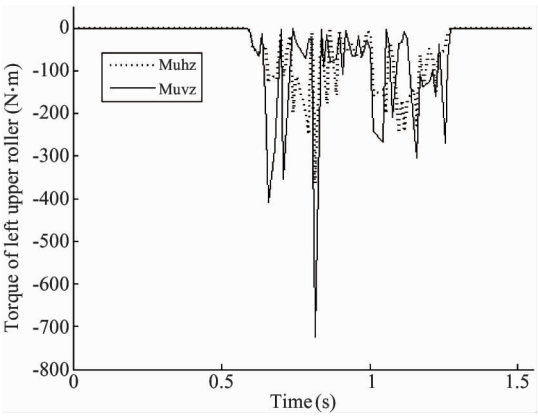

Fig. 4 Torque of left upper roller

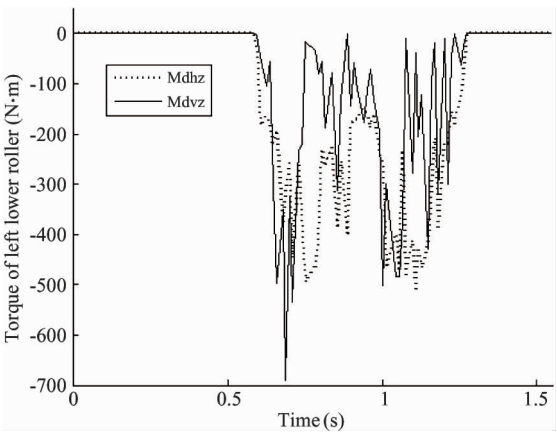

Fig. 5 Torque of left lower roller

As an input, the forming torque in left upper and lower roller can be obtained as shown in Fig. 4 and Fig. 5.

Meanwhile the counter-force of the left upper and lower roller also can be obtained as shown in Fig. 6 and Fig. 7.

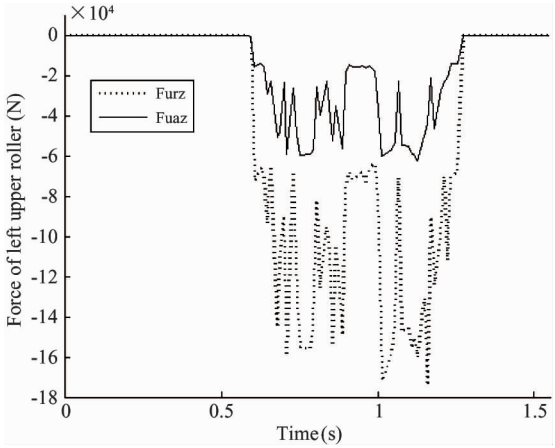

Fig. 6 Counter-force of left upper roller

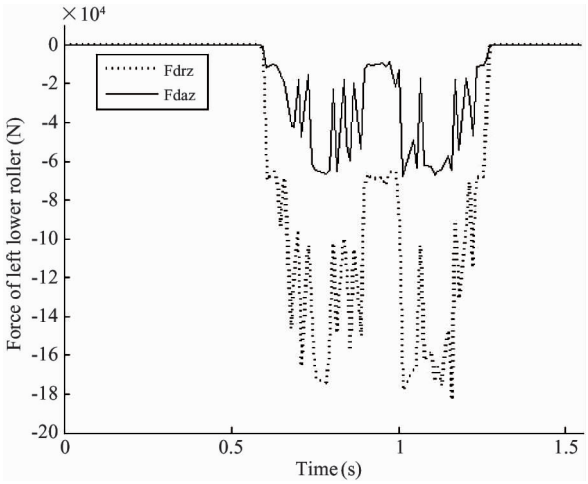

Fig. 7 Counter-force of left lower roller

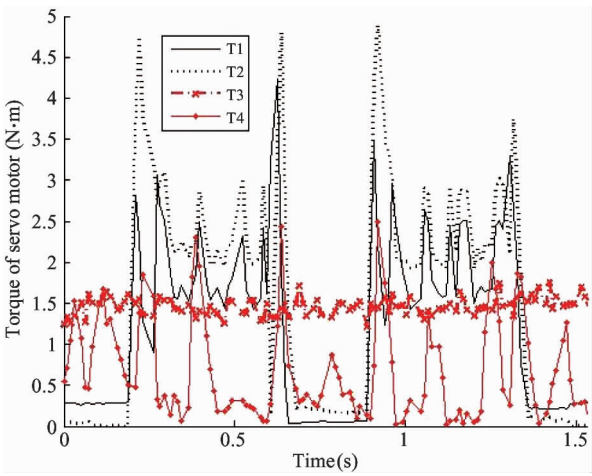

Fig. 8 Torque of servo-motor

The curves of the torque of the servo-motor with the change of time t are shown as Fig. 8.

Based on the actual 3D roll forming machine as

Fig. 1, the motor and mechanism parameters are calculated as Table 1 shows.

Table 1 Motor and mechanism parameters

parameters	value
rotor inertia moment of servo motor J_{dj1}, J_{dj2}, J_{dj3}, J_{dj4} (kg·m^2)	0.0026
inertia moment of servo motor reducer J_{js1}, J_{js2}, J_{js3}, J_{js4} (kg·m^2)	0.00076
moving servo motor reducer speed ratio i	20
inertia moment of ball screw J_{sg1}、J_{sg2} (kg·m^2)	0.007
lead of ball screw h (m)	0.008
reference radius of gear r (m)	0.132
inertia moment of gear J_{cl} (kg·m^2)	0.27
mass of rotating spindle m_{zz} (kg)	263.4
inertia moment of rotating spindle J_{zz} (kg·m^2)	0.02
mass of screw seat components m_{zs}、m_{ys} (kg)	35.3
mass of rotating frame assembly m_{xj} (kg)	422.32
inertia moment of rotating frame assembly J_{xj} (kg·m^2)	36.36
inertia moment of upper and lower roller axle J_{uz}、J_{dz} (kg·m^2)	0.0044
inertia moment of upper roller J_{ug} (kg·m^2)	0.0326
inertia moment of lower roller J_{dg} (kg·m^2)	0.031

Roller load and the parameters shown in Table 1 are substituted in Eq. (6), and the software MATLAB 6.5 is used to calculate and draw the curves of angular acceleration to time. The actual angular acceleration of the servo-motors can be obtained in the variable cross section roll-forming process of 1.5mm thick and TRIP600 high strength steel sheet shown as Fig. 9.

By the method of integration, the curve of motor angular velocity in time domain can be obtainid shown here as Fig. 10.

4 Conclusions

In this paper, the kinetic energy of one stand dynamical model of 3D roll forming machine is applied to the Lagrange equations and then the dynamical equations of this system is deduced. The conclusions are drawn as follows:

(1) It's feasible that the dynamic equations of the eight degrees freedom double racks gear 3D roll forming machine is built with the method of Lagrange equation, and the analytical solutions of system servo motor's angular acceleration and angular velocity can be obtained by solving equation groups.

(2) The fact applying the calculated angular acceleration and angular velocity into the variable cross section roll forming process of 1.5mm thick TRIP600 high strength steel sheet with the conditions of 3m/s feeding speed reveals that the results obtained comes to the agreement with that of the practical roll forming process, suggesting this method would provide the theoretical basis for the design of 3D roll forming machine and development of control system.

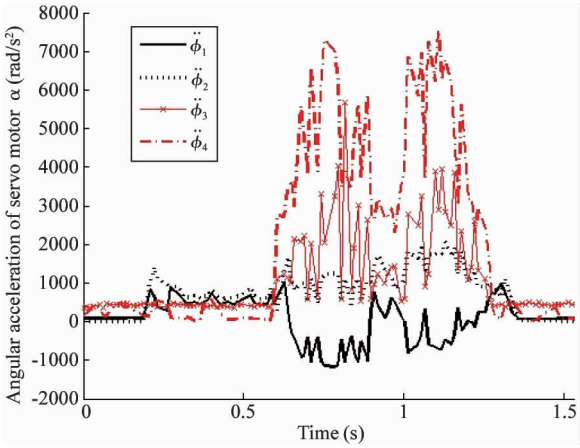

Fig. 9 Angular acceleration of servo motor

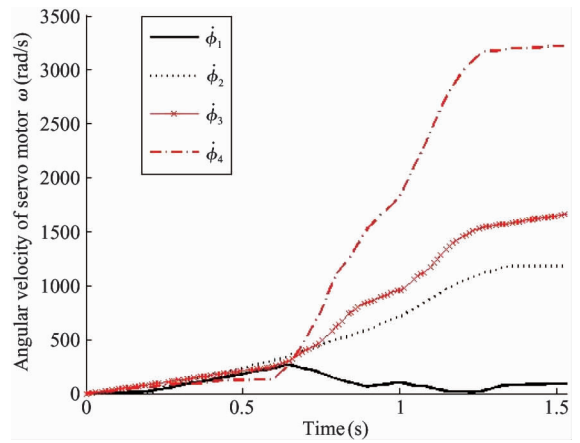

Fig. 10 Angular velocity of servo motor

References

[1] Nefussi G, Proslier G, Gilormini P. A simulation of cold-roll forming for elastoplastic materials. *Int J Mech Sci*, 1998, 40(1): 15-25

[2] Larra J N, Galdos1 L, Uncilla1 L, et al. Development and validation of a numerical model for sheet metal roll forming. *Int J Mater Form*, 2010, 3 (1): 151-154

[3] Paralikas J, Salonitis K, Chryssolouris G. Investigation of the effects of main roll-forming process parameters on quality for a V-section profile from AHSS. *Int J Adv Manuf Tech*, 2009, 44 (3): 223-237

[4] Bui Q V, Ponthot J P. Numerical simulation of cold roll forming processes. *Journal of Materials Processing Technolog*, 2008, 202 (1): 275-282

[5] N. Kim, S I Oh. Analysis tool for roll forming of sheet metal strips by the finite element method. *CIRP Annals - Manufacturing Technology*, 1999, 48 (1): 235-238

[6] Heislitz F, Livatyali H, Ahmetoglu M A, et al. Simulation of roll forming process with the 3-D FEM code PAM-STAMP. *Journal of Materials Processing Technology*, 1996, 59 (1-2): 59-67

[7] Zeng J, Liu Z H, Champliaud H. FEM dynamic simulation and analysis of the roll-bending process for forming a conical tube. *Journal of materials processing technology*, 2008, 198 (1-3): 330-343

[8] Cai Z Y, Sui Z, Cai F X, et al. Continuous flexible roll forming for three-dimensional surface part and the forming process control. *Int J Adv Manuf Technol*, 2013, 66 (1-4): 393-400

[9] Paralikas J, Salonitis K, Chryssolouris G. Optimization of roll forming process parameters: a semi-empirical approach. *Int J Adv Manuf Technol*, 2010, 47 (9-12): 1041-1052

[10] Moen C D, Igusa T, Schafer B W. Prediction of residual stresses and strains in cold-formed steel members. *Thin-Walled Structures*, 2008, 46 (11): 1274-1289

[11] Zeng G, Li S H, Yu Z Q, et al. Optimization design of roll profiles for cold roll forming based on response surface method. *Materials and Design*, 2009, 30 (6): 1930-1938

[12] Yang Y Y, Jin D W. Mechanical System Dynamics. Beijing: Tsinghua University press, 2009. 7-10 (In Chinese)

[13] Wen X S, Qiu J, Tao J Y. Analysis Dynamics and Application of Electromechanical Systems. Beijing: Science Press, 2003. 32-61 (In Chinese)

[14] Wang Z F. Analytical Mechanics. Beijing: Science Press, 2002. 47 (In Chinese)

Na Risu, born in 1976. She received her M. S. degree from College of Sciences, Inner Mongolia University of Technology in 2004. She received her Ph. D degree in College of Sciences, Inner Mongolia University of Technology in 2014. Her research focus on dynamics of mechanical systems.